ChemPubSoc Europe

DOI: 10.1002/chem.201503171

CHEMISTRY
A European Journal
Full Paper

Domino Reactions

Microwave-Assisted Organocatalyzed Rearrangement of Propargyl Vinyl Ethers to Salicylaldehyde Derivatives: An Experimental and Theoretical Study

David Tejedor,*[a] Leandro Cotos,[a] Daniel Márquez-Arce,[a] Mikel Odriozola-Gimeno,[b] Miquel Torrent-Sucarrat,[b, c] Fernando P. Cossío,[b] and Fernando García-Tellado*[a]

Abstract: The microwave-assisted imidazole-catalyzed transformation of propargyl vinyl ethers (PVEs) into multisubstituted salicylaldehydes is described. The reaction is instrumentally simple, scalable, and tolerates a diverse degree of substitution at the propargylic position of the starting PVE. The generated salicylaldehyde motifs incorporate a broad range of topologies, spanning from simple aromatic monocycles to complex fused polycyclic systems. The reaction is highly regioselective and takes place under symmetry-breaking conditions. The preparative power of this reaction was demonstrated in the first total synthesis of morintrifolin B, a benzophenone metabolite isolated from the small tree *Morinda citrifolia* L. A DFT study of the reaction was performed with full agreement between calculated values and experimental results. The theoretically calculated values support a domino mechanism comprising a propargyl Claisen rearrangement, a [1,3]-H shift, a [1,7]-H shift (enolization), a 6π electrocyclization, and an aromatization reaction.

Introduction

Propargyl vinyl ethers (PVEs) **1** are a privileged group of small-size, densely functionalized, and readily accessible linear scaffolds. The main key to the chemical reactivity encoded in these structures is the [3,3]-sigmatropic rearrangement (propargyl Claisen rearrangement) shown in Scheme 1 A,[1] which takes place irreversibly and under thermodynamic control to generate the allene **2**.[2] Since the first, seminal thermally driven rearrangement achieved by Black and Landor in 1965,[3] which served to determine that propargylic systems could be accommodated into the Claisen rearrangement, a vast number of propargyl Claisen rearrangements have been successfully performed.[1] The main drawback of these rearrangements is the requirement for high temperatures, which forced the use

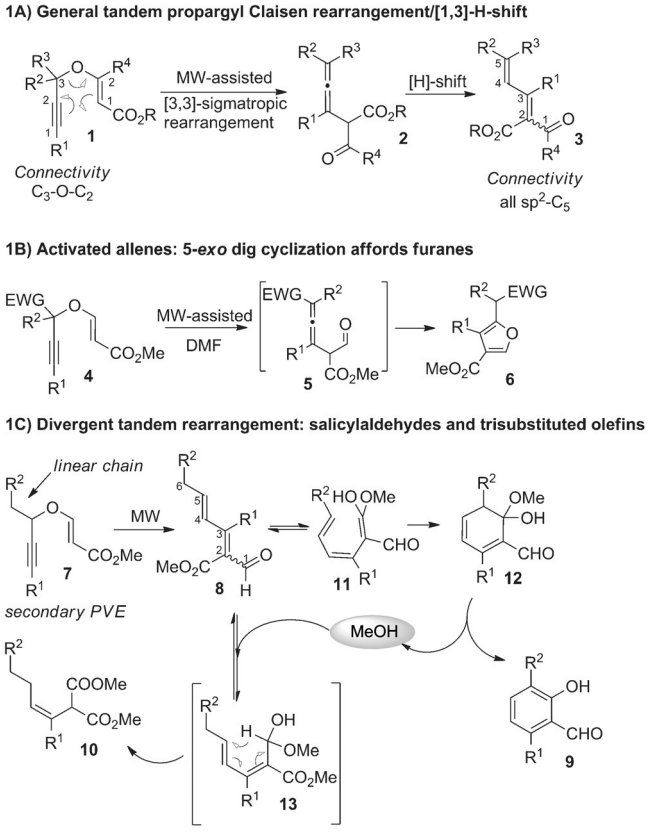

Scheme 1. The MW-assisted propargyl Claisen rearrangement of propargyl vinyl ethers **1**. EWG = electron-withdrawing group.

[a] *Dr. D. Tejedor, Dr. L. Cotos, D. Márquez-Arce, Dr. F. García-Tellado*
Departamento de Química Biológica y Biotecnología
Instituto de Productos Naturales y Agrobiología
Consejo Superior de Investigaciones Científicas
Avenida Astrofísico Francisco Sánchez 3
38206 La Laguna, Tenerife (Spain)
E-mail: fgarcia@ipna.csic.es
dtejedor@ipna.csic.es

[b] *M. Odriozola-Gimeno, Dr. M. Torrent-Sucarrat, Prof. F. P. Cossío*
Facultad de Química
Universidad del País Vasco-Euskal Herriko Unibertsitatea (UPV/EHU)
and Donostia International Physics Center (DIPC)
P. K. 1072, San Sebastian-Donostia (Spain)

[c] *Dr. M. Torrent-Sucarrat*
Ikerbasque, Basque Foundation for Science
María Díaz de Haro 3, 6°, 48013 Bilbao (Spain)

Supporting information for this article is available on the WWW under http://dx.doi.org/10.1002/chem.201503171.

of high-boiling solvents and harsh conditions. These experimental difficulties prevented their use in preparative organic synthesis, in sharp contrast to the counterpart involving allyl vinyl ethers.[4] However, this scenario dramatically changed in the last decade with the emergence of milder metal-catalyzed protocols[5] and the replacement of conventional heating with laboratory microwave (MW) equipment.[1] Under MW heating, allenes **2** rearrange to the more stable diene derivatives **3** through a pseudo-pericyclic [1,3]-H shift (Scheme 1 A). Overall, this tandem rearrangement transforms a C_3-O-C_2 linear structure, easily assembled through C–O bond-forming chemistry, into an all-sp^2-linear C_5 carbogenic block[6] armed with a reactive carbonyl group (aldehyde or ketone), an ester group, and a doubly conjugated diene. An exception to this outcome is represented by the activated allenes **5** (EWG = ester or secondary amide),[7] which directly rearrange to the furan derivatives **6** through a tandem enolization/O cyclization/H transfer process (Scheme 1 B).[8]

A particularly striking reactivity profile arises from monosubstituted PVEs **7** (R^3 = H, hereinafter referred to as secondary PVEs) bearing a linear chain at the propargylic position (Scheme 1 C). In these cases, the rearrangement affords a roughly equimolar mixture of salicylaldehyde **9** and trisubstituted olefin **10**.[9] The formation of salicylaldehyde **9** can be formally rationalized through a tandem enolization/6π electrocyclization/aromatization process with the net generation of a methanol molecule per molecule of salicylaldehyde. On the other hand, the stereoselective formation of the trisubstituted olefin **10** should be mediated by the formation of the hemiacetal **13** to launch an internal redox process involving a [1,5]-H shift. Overall, this manifold is a divergent chemical process that can produce two well-differentiated products from the same reactive intermediate and through two interconnected pathways (the product of one pathway launches the other). Remarkably, the manifold could be selectively funneled toward each of these two products by careful design of the experimental conditions. Thus, salicylaldehydes **9** could be cleanly obtained in 60–80% yield by MW irradiation of a xylene solution of PVEs **7** in the presence of 4 Å molecular sieves (MS) (300 mg per mole substrate).[9] Although initially we used 4 Å MS as additive, we later discovered that pyridine (200 mol%) could replace the MS, rendering the process homogenous and easier to perform.[10] It was assumed that the beneficial action of the two additives was related to a reduction of the activation barrier for the enolization process, otherwise the limiting step of the process. Although this is an uncommon reactivity for MS, there are some precedents for their use in enolization processes.[11] On the other hand, the MW irradiation of a methanolic solution of PVEs **7** exclusively afforded the olefin derivatives **10** in good to excellent yields (75–95%) and with complete stereoselectivity (the two alkyl chains are located in *trans* positions).[12]

The salicylaldehyde motif is an important building block for the preparation of numerous pharmacologically relevant coumarins,[13a] flavonoids,[13b] chromenes,[13c,d] catechols,[13e] and several mycotoxins,[13f] as well as chiral catalysts based on transition metal Schiff base complexes (salen catalysts).[14] Salicylaldehydes are commonly prepared by direct formylation of the corresponding phenol derivatives[15] under the classical Reimer–Tiemann conditions ($CHCl_3$/KOH)[15a] or the Duff procedure (hexamethylenetriamine/acetic acid /sulfuric acid).[15b,c] Interestingly, the 3,6-disubstitution pattern present in salicylaldehydes **9** cannot be easily accessed by using these standard protocols. Among other drawbacks, these reactions have regioselectivity problems when the *ortho* and *para* positions to the hydroxyl functionality are not conveniently blocked.[16]

The efficiency and instrumental simplicity of this reaction together with the importance of the salicylaldehyde motif prompted us to undertake a systematic study of this reaction with the aim of transforming it into a general, robust, and preparative protocol for accessing salicylaldehyde-based structural motifs. The transformation of this reaction into a standard synthetic protocol with preparative value (academic and industrial) required implementation of a catalytic version incorporating the following: 1) the use of a cheap and easy handled catalyst (additive); 2) high tolerance to broad and diverse substitution patterns on the PVE; and 3) bench-friendly reaction processing. We report herein how these conditions could be met by using imidazole (10 mol%) as a basic catalyst and how this catalytic manifold could be used for the construction of salicylaldehyde motifs supported on a broad range of topologies, which spanned from simple aromatic monocycles to complex fused polycyclic systems. We also performed a theoretical study on this reaction that is in full agreement with the observed experimental results. Finally, the preparative power of this reaction has been demonstrated in the first total synthesis of morintrifolin B,[17] a benzophenone metabolite isolated from the small tree *Morinda citrifolia* L.

Results and Discussion

Catalytic synthesis of 3,6-disubstituted salicylaldehydes from secondary PVEs

Although pyridine had proved to be a convenient additive for this transformation,[10] the large excess required (200 mol%) precluded its use in large-scale preparative reactions. Guided by the current principles of sustainable chemistry,[18] we searched for new additives to be used as true catalysts. For this study, we chose the transformation of PVE **7a** into salicylaldehyde **9a** (Table 1). We had observed in earlier studies[9,10] that the substitution pattern of this PVE was one of the worst tolerated by this reaction with both 4 Å MS (43%)[9] and pyridine (53%).[10] Because the use of pyridine improved the efficiency of the reaction by 10%, we envisioned that this reaction could be a convenient benchmark for the assay of other basic additives better suited than pyridine to catalyze the required enolization of dienal **8** to intermediate **11** (Scheme 1 C). With this idea in mind, we assayed the bases shown in Table 1 (entries 1–15). Additionally, we assayed a set of common acids of moderate strength to see if they could also be suitable additives for this reaction (Table 1, entries 16–18). The reactions were performed under our previously established conditions [xylene (1 mL), MW (300 watt, 200 °C, and closed vessel), 1 h]

Table 1. Optimization of the additive for the MW-assisted synthesis of salicylaldehyde **9a**.

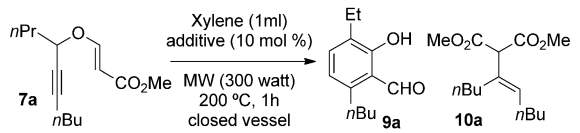

Entry	Additive[a]	pK_a[b]	**9a** + **10a** [%]	Ratio **9a**/**10a**[c]
1	DABCO	2.97	64	1.5
2	aniline	4.63	35	0.17
3	DMBA	4.68	36	0.16
4	pyridine[d]	5.2	87	1.6
5	imidazole	6.9	84	1.7
6	collidine	7.4	68	1.4
7	DMAP	9.2	78	2.1
8	DIPEA	10.8	64	1.4
9	quinuclidine	11	44	0.8
10	DBU	12	62	1.5
11	*t*BuOK	17	37	0.3
12	indole	21[e]	34	0.1
13	pyrrole	23[e]	34	0.1
14	urea	26.9[e]	42	0.7
15	TMP	37[e]	74	1.8
16	$C_6H_6CO_2H$	4.2	58	0.8
17	$C_5H_{10}NH_2^+AcO^-$	8.7	56	0.6
18	phenol	9.95	55	0.1
19	4 Å MS[f]		90	1

[a] Abbreviations: DMBA: 1,3-dimethylbarbituric acid; DMPA: 4-dimethylaminopyridine; DIPEA: *N*,*N*-diisopropylethylamine; DBU: 1,8-diazabicyclo[5.4.0]undec-7-ene; TMP: 2,2,6,6-tetramethylpiperidine. [b] In H_2O. [c] Determined by NMR spectroscopy. [d] 200 mol%. [e] In DMSO. [f] 300 mg mmol^{-1}.

with a catalytic amount (10 mol%) of additive. Imidazole and 4-(*N*,*N*-dimethylamino)pyridine proved to be the best additives (Table 1, entries 5 and 7), with the highest yields (84 and 78% combined yield) and **9a/10a** ratios of 1.7 and 2.1, respectively. The yields and ratios were in both cases similar to those obtained with an excess of pyridine (Table 1, entry 4) and substantially better than those obtained with 4 Å MS (90% combined yield, 1:1 ratio, Table 1, entry 19). Practical reasons (price and availability) made imidazole the preferred catalyst for this reaction. The use of acid additives had the reverse effect, generating the olefin **10a** as the main product, albeit with moderate efficiency (Table 1, entries 16–18).

The scope and efficiency of the catalytic manifold was first studied with the transformation of the secondary PVEs **7a**–**g** into the corresponding salicylaldehydes **9a**–**g** (Scheme 2).[19] In general, the reaction delivered the corresponding salicylaldehydes **9a**–**f** in moderate to good yields (54–72%) depending on the substitution pattern of the PVE. Esters, isolated double bonds, and protected hydroxyl groups were well tolerated. Interestingly, the PVE **7g** bearing an electron-rich alkyne in its structure could be also transformed into the corresponding hydroxylated salicylaldehyde **9g** (38%). In spite of this moderate-to-low yield, the importance of hydroxylated aromatic platforms[20] and the potential use of hydroxylated salicylaldehydes as convenient building blocks for accessing biologically relevant compounds[13,21,22] ensures a preparative value for this transformation. In addition, the easy and direct access to secondary PVEs containing the ethoxyacetylene motif (ethoxyacetylene is commercial available) allows for fast access to a broad range of 3-substituted 6-ethoxysalicylaldehyde platforms.

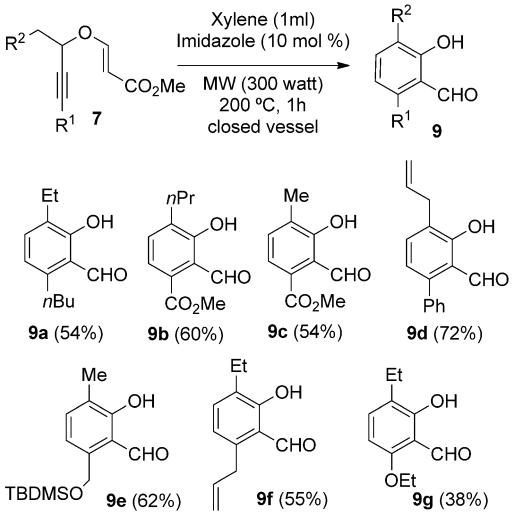

Scheme 2. Imidazole-catalyzed synthesis of salicylaldehydes **9** from secondary propargyl vinyl ethers **7**.

Catalytic synthesis of 3,4,6-trisubstituted salicylaldehydes from tertiary PVEs

Once the catalytic version of the reaction had been standardized, we studied its extension to PVEs **1** bearing two substituents at the propargylic position (R^2 and $R^3 \neq H$, hereinafter referred to as tertiary PVEs). The main advantages associated with the incorporation of tertiary PVEs into the reaction manifold are related to: 1) skeletal complexity: the use of cyclic ketones (mono- or polycycles, simple or fused) should increase the power of the manifold to generate structural complexity and topological diversity; 2) reactivity: the presence of two substituents on the propargylic position of the tertiary PVE should favor both the propargyl Claisen rearrangement[1] and the enolization process (see Scheme 1C), which should translate into a net increase in the reaction efficiency. With these ideas in mind, we prepared an extensive set of tertiary PVEs **1**[23] incorporating a wide array of substituents and molecular topologies (Scheme 3). These PVEs were conveniently prepared from the corresponding tertiary propargyl alcohols and methyl propiolate according to our recently reported protocol.[24]

In general, tertiary PVEs proved to be excellent substrates for this catalytic reaction affording the corresponding aromatic derivatives in good average yield. The PVEs **1a**–**d**[23] derived from acyclic ketones delivered the corresponding aromatic derivatives **14a**–**d** in good average yield and incorporated varied substitution patterns at the aromatic ring, including alkyl, aryl, and oxygen-containing substituents. Remarkably, the last-named functional groups are introduced with high efficiency (**14a**, 73%) and in a chemo-differentiated manner (one as a free OH, the another as a protected OH group). This property enables orthogonal manipulation of each hydroxyl group at

the aromatic ring without taking special precautions or using special reagents. An interesting aspect of this reaction is the breakage of the symmetry observed when symmetrically disubstituted PVEs (ketones) are used ($CH_2R^2=R^3$). In these cases, the reaction places the R^3 substituent at the C^5 position of the ring, delivering the R^2 substituent (the sec-alkyl chain) at the corresponding C^6 position. This is a very important property and it allows the final differentiation of the otherwise identical propargylic substituents of the PVE, which increases the diversity-generating power of the reaction manifold. The derivative **14d** is a good example of this symmetry-breaking chemical differentiation ($R^3=$Et, $R^2=$Me).

The tertiary PVEs **1e**–**u**,[23] derived from symmetrical monocyclic ketones, were also convenient substrates for the reaction and provided a broad set of fused bicyclic salicylaldehyde derivatives featuring varied aromatic functionalization. Thus, the PVEs **1e**–**o**, armed with a cyclohexane motif, delivered the corresponding 1-hydroxy-5,6,7,8-tetrahydronaphthalene-2-carbaldehydes **14e**–**o** adorned with a wide array of substituents at the C^3 position. The substituents ranged from simple hydrogen, the worst case (**14k**, 17%), to heteroatoms including silicon (**14j**, 85%), bromine (**14l**, 47%), oxygen (**14m**, 77%), and nitrogen (**14o**, 93%). The low yield of **14k** is in accordance with our previous results using 4 Å MS[9] or pyridine[10] and confirms that substitution at the terminal alkyne position ($R^1\neq$H) is necessary to favor the formation of the enol intermediate **11** (see Scheme 1C). Thus, the high efficiency of this reaction when a bulky *tert*-butyl group is located at the terminal position of the triple bond in the parent PVE (**14h**, quantitative) is remarkable. The substitution of this group by less sterically demanding groups (*n*-Bu, Me) lowered the yield (54 and 55%, respectively). On the other hand, generation of the salicylaldehyde **14p** (31%) incorporating a fused cyclobutene ring is outstanding and reflects the potential of this catalytic reaction to generate molecular topologies not easily accessible by other methods.[25]

Other topologies based on the bicyclo[*n*.4.0] motive ($n=3$, 5, and 10) were explored. The reaction proved to be general with regard to the size of the non-aromatic ring (**14p**–**s**). An interesting case was offered by the derivative **14s** incorporating a C_{12} ring in its structure. These topologies incorporating sp^3-rich macrocycles are highly appreciated and underexploited structural motifs for drug discovery.[26] The reaction also allowed efficient access to C^6-substituted 8-hydroxy-1,2,3,4-tetra-

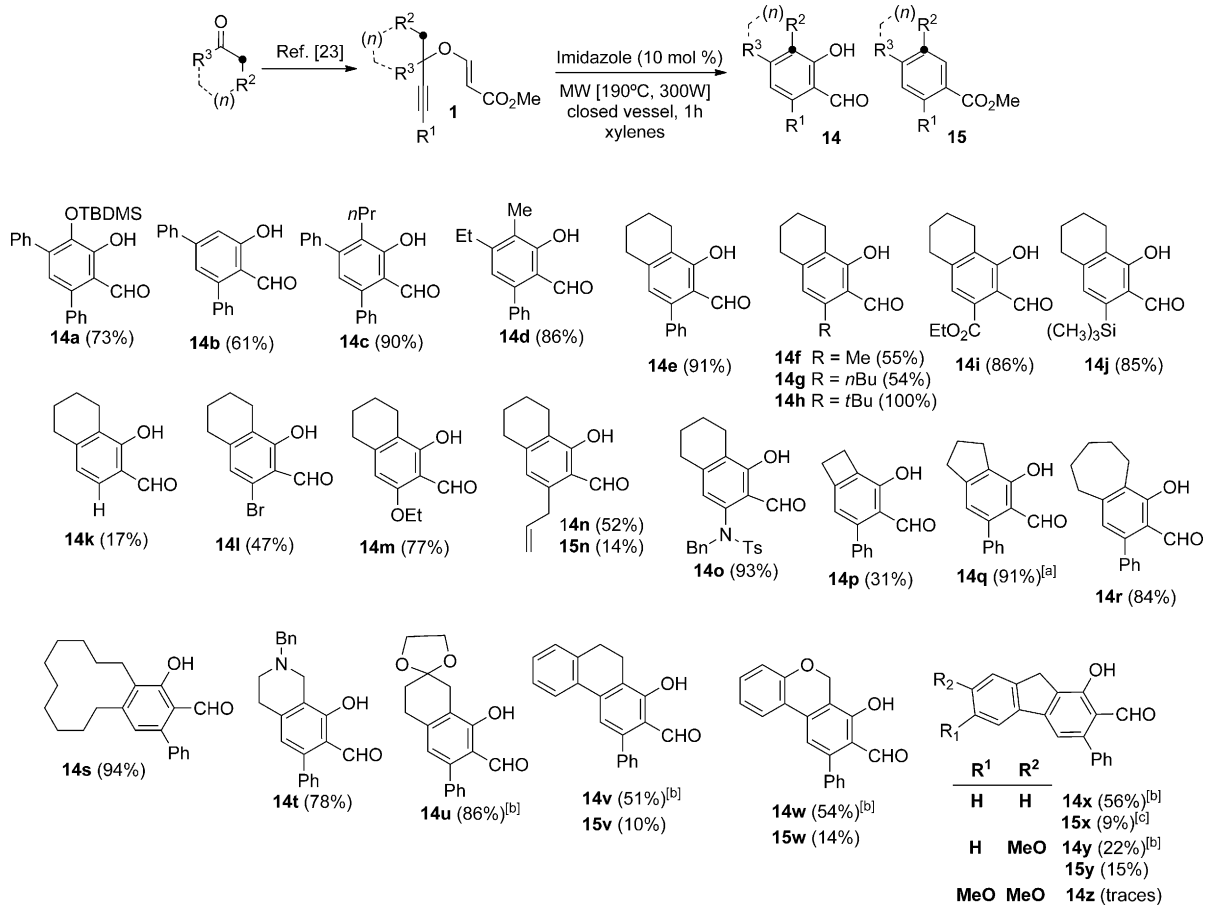

Scheme 3. Imidazole-catalyzed synthesis of salicylaldehydes **14** from tertiary propargyl vinyl ethers **1**. [a] The reaction was performed on a gram scale (1.1 g, 4.4 mmol). [b] The corresponding PVEs were not isolated. Yields refer to the two-step process: formation of the PVE from the corresponding propargyl alcohol and MW-assisted rearrangement. See the Experimental Section and the Supporting Information for details. [c] The yield was assigned by quantitative NMR integration of the crude reaction residue.

hydroisoquinoline-7-carbaldehydes (**14t**, 78%) and 1-hydroxy-5,6,7,8-tetrahydronaphthalene-2-carbaldehydes bearing a protected ketone at C^7 as a convenient handle for further ring functionalization (**14u**, 86%). Both structures are interesting scaffolds for medicinal chemistry.[27] Salicylaldehydes **14v–z** are examples of fused tricyclic structures with natural-product-like topologies.[28] Interestingly, in these cases, the formation of salicylaldehydes **14** is accompanied by formation of the corresponding benzoate derivatives **15**, which could stem from the 6π electrocyclization/aromatization processes of another diene **2** conformation arising from ketone–ester group interchange (see below). The subtle influence of the ketone skeleton on the selectivity of the reaction was apparent from the somehow surprising formation of the benzoate derivative **15n**, the only benzoate detected in the mono- and bicyclic series. An subtle electronic effect was also observed in the reactions involving fused bicyclic ketones. Whereas the formation of the 9*H*-fluorene derivatives **14x–z** showed a clear deterioration of the reaction efficiency with increasing electron richness of the aromatic ring (compare **14x** with **14y** and **14z**), the presence of an oxygen atom at the 9-position of the 9,10-dihydrophenantrene core was irrelevant in terms of efficiency, but not in terms of selectivity (compare **14v**/**15v** and **14w**/**15w**).

The reaction proved to be highly regioselective when asymmetrically substituted tertiary PVEs (ketones) were used (Scheme 4). Thus, PVE **1aa** bearing two different alkyl substituents at the propargylic position (R^2 = Et, R^3 = Me) delivered the salicylaldehyde **14aa** in 63% yield (19:1 isomeric ratio). The reaction manifold selectively incorporated the more substituted homopropargylic carbon atom into the final aromatic ring. Exquisite regioselectivity was also observed in the synthesis of the derivative **14ab** (86%, 50:1 isomeric ratio), showing a clear preference for the benzylic position over the alternative one. The observed regioselectivity could be explained by the relative stabilities of the isomeric trienol intermediates (see below; Scheme 4, inset), which in turn relies on the relative stability of the terminal double bonds.

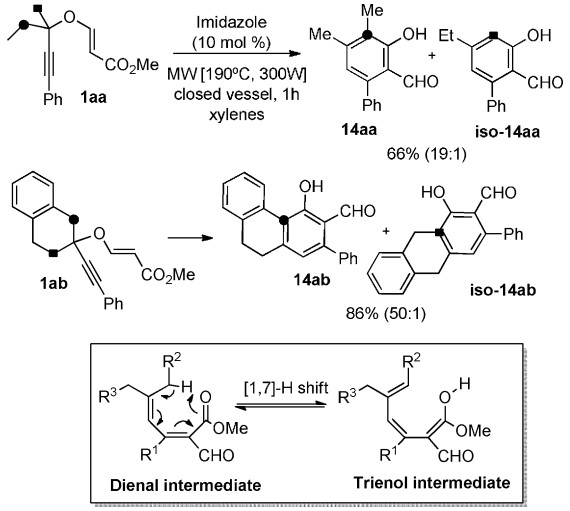

Scheme 4. Regioselectivity in the imidazole-catalyzed reaction.

Application to the first total synthesis of morintrifolin B

The easy access to these multisubstituted salicylaldehydes scaffolds gave us the opportunity to use them as convenient starting materials for the synthesis of more complex structures embodying the parent aromatic ring. Among the possible structures, we chose benzophenones because of their chemical and biological relevance.[29] The family of natural benzophenones has more than 300 members with great structural diversity and bioactive properties including antifungal, anti-HIV, antimicrobial, antioxidant, and antiviral activity.[30] Morintrifolin B (**19**)[17] is a naturally occurring benzophenone isolated from the small tree *Morinda citrifolia* L. (Rubiaceae), commonly known as noni and widely distributed in southern Asia and the Pacific islands. The plant has found popular medicinal use for the treatment of asthma, bone fractures, cancer, cholecystitis, dysentery, lumbago, menstrual cramps, urinary difficulties, and many other ailments.[31] In spite of the pharmacological potential offered by the constituents of the plant, there are no reports to date on synthetic or biological studies on morintrifolin B. Because of our interest in this kind of compounds, we undertook a short synthesis of this benzophenone metabolite from the salicylic acid derivative **16** (Scheme 5), readily available from salicylaldehyde **9c** by simple phenol protection (BrBn, K_2CO_3, acetone, 93%) and aldehyde oxidation ($NaClO_2$, sulfamic acid, THF/H_2O, 87%). The trifluoroacetic anhydride-mediated reductive coupling with the 2-methoxy resorcinol derivative **17** assembled the benzophenone core of **19**, which was subjected to selective deprotection (H_2, Pd/C) to give the intermediate **18** (49% for two steps) featuring the same hydroxylation pattern as the target natural product. Finally, the acid-controlled transesterification of this intermediate with ethylene glycol afforded morintrifolin B (**19**) in 80% yield. The five-step synthesis delivered morintrifolin B in an overall yield of 32% from the corresponding propargyl vinyl ether **7c**. The

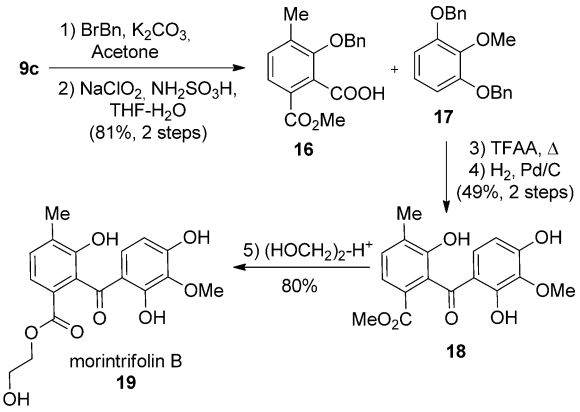

Scheme 5. Short synthesis of morintrifolin B.

synthetic extension to other structurally related benzophenones and studies on their biological activity are in progress.

Computational studies on the reaction mechanism

To provide new insight into the reaction mechanism for the rearrangement of the propargyl vinyl ethers, we performed a computational DFT study using a simplified model denoted **R** in Scheme 6, where $R^1=R^2=R^4=H$ and $R^3=CH_3$. Some hydrogen-transfer processes (enolization and [1,3]-H shifts) show unrealistically[32] high free-energy barriers (ca. 55 kcal mol^{-1}). In these cases one imidazole molecule can act as a catalyst by taking advantage of its amphoteric character. The names of these stationary points end with "**-Imz**" to indicate the use of a molecule of imidazole as a suitable additive. All stationary points on the potential surface were fully optimized with the hybrid density functional B3LYP[33] and the 6-311+G(d,p) basis set.[34] Harmonic analyses were performed at this level of theory to verify the nature of the corresponding stationary points (minima or transition states), as well as to provide the zero-point vibrational energy and the thermodynamic contributions to the enthalpy and free energy for $T=298$ K. Moreover, intrinsic reaction coordinate[35] calculations were performed to ensure that the transition states connect the reactants and products belonging to the reaction coordinate under study. The final energies were obtained by performing single-point M06-2X[36] calculations with the 6-311+G(d,p) basis set at the optimized B3LYP geometries. The average difference between the B3LYP and M06-2X increments of energy was 3.1 kcal mol^{-1}. The raw data obtained with the B3LYP and M06-2X results are reported in the Supporting Information (see Tables S1–S5 in the Supporting Information) along with the Cartesian coordinates of each stationary point (see Table S6 in the Supporting Information). The values discussed in the text and the values reported in Schemes 6 and 7 are relative free energies evaluated at the M06-2X/6-311+G(d,p)//B3LYP/6-311+G(d,p) level of theory. All quantum chemistry calculations in this work were carried out with the Gaussian 09 program package.[37] The complete list of energies is reported in Tables S1–S5 of the Supporting Information. Exhaustive potential-energy surface scans with all the reaction mechanisms studied and selected geometrical parameters are shown in Figures S1–S15 of the Supporting Information. The transition states and intermediates of the studied domino rearrangement show several conformers with very similar energies (e.g., rotation about sp^3 carbon atoms and isomerization of double bonds).

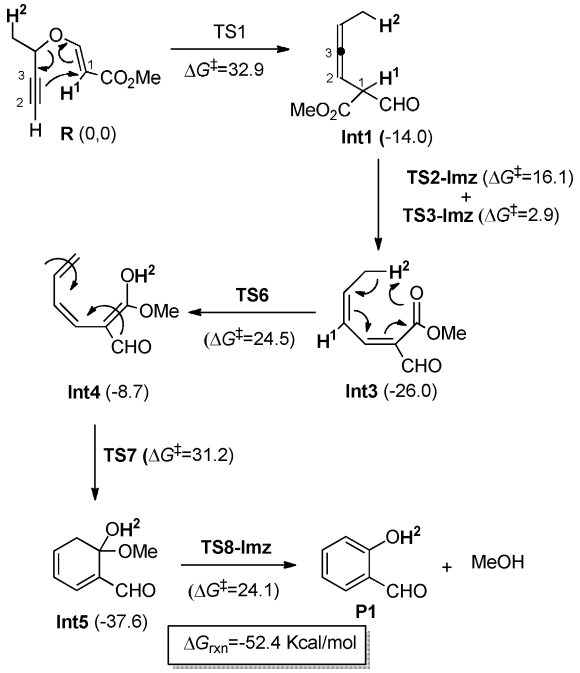

Scheme 6. Reaction pathway for the domino process leading to the formation of salicylaldehyde derivative **P1**. Transition-state descriptors denoted **TS-Imz** refer to saddle points assisted by a molecule of imidazole (see text). Relative free energies are given in kcal mol^{-1}.

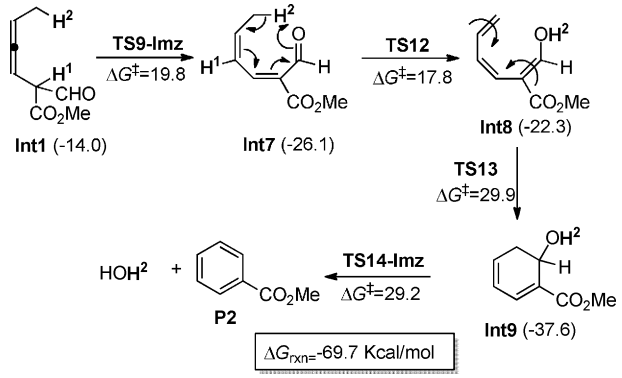

Scheme 7. Reaction mechanism for the domino process leading to the formation of methyl benzoate **P2**. Transition states including the **Imz** descriptor refer to saddle points assisted by a molecule of imidazole (see text). Relative free energies are given in kcal mol^{-1}.

The domino reaction starts with a thermally allowed [3,3]sigmatropic process of **R** to yield **Int1** (Scheme 6). This propargyl Claisen rearrangement shows an activation free energy barrier (**TS1**) of 32.9 kcal mol^{-1}, which is the highest activation energy along the alternative reaction paths (see below). As expected, **TS1** involves the cleavage and formation of a C–O and a C–C bond, respectively, as well as the conversion of a propargyl and an enol group into an allene and a carbonyl group, respectively (Figure 1 and Figure S1 of the Supporting Information). Allenyl intermediate **Int1** lies about 14 kcal mol^{-1} below **R**. Several conformations of **Int1** can be considered, and in this work we calculated six of them (**Int1a** to **Int1f**) with very similar relative energies (differences smaller than 2 kcal mol^{-1}, see the Supporting Information).

The next step of the domino process consists of conversion of allene **Int1** to unsaturated ester **Int3** (Scheme 6). This process formally corresponds to a thermal antarafacial [1,3] sigmatropic shift involving hydrogen atom H^1 and allyl scaffold C^1–C^3. The direct process is not geometrically favored, since the activation energy for this direct process is about 63 kcal mol^{-1}

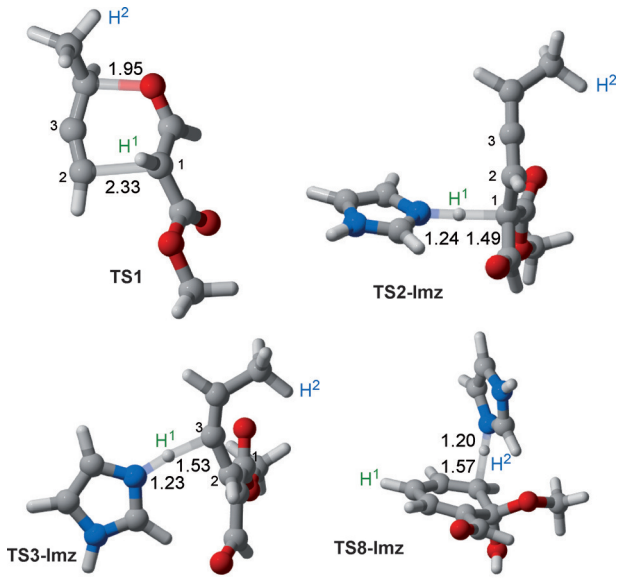

Figure 1. Fully optimized structures of saddle points **TS1** associated with [3,3] propargyl Claisen rearrangement, **TS2-Imz** and **TS3-Imz** corresponding to [1,3] hydrogen shift, and **TS8-Imz** associated with the aromatization process (see Scheme 6). Bond lengths are given in ångstrom.

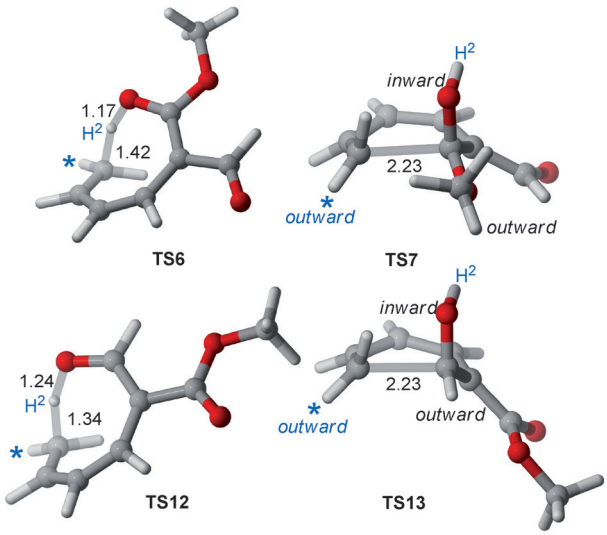

Figure 2. Fully optimized structures of saddle points **TS6**,**12**, associated with [1,7] sigmatropic shifts, and **TS7**,**13**, corresponding to [$\pi 6_d$] electrocyclizations (see Scheme 6 and Scheme 7). Bond lengths are given in ångstrom. Stars indicate the position of R^2 groups in more substituted transition structures (see Scheme 4).

(see the Supporting Information). However, our calculations indicate that this 1,3-prototropy is feasible under imidazole assistance. Thus, imidazole can remove proton $\mathbf{H^1}$ from **Int1** via **TS2-Imz** and transfer it to C^3 via **TS3-Imz** (see Figure 1 and the Supporting Information for additional details) with overall activation energy of about 20 kcal mol^{-1}, since the intermediate ion pair is almost isoenergetic with **TS3-Imz**. An alternative route involving the corresponding enol-allene intermediates **Int2** via tautomeric equilibria involving one molecule of imidazole can be also considered (see **TS4**, **TS5**, and **TS4-Imz** in Figures S3 and S6 of the Supporting Information).

Oxatriene **Int3** can be transformed into triene **Int4** via a thermally allowed antarafacial [1,7] sigmatropic shift. It is noteworthy that the geometry of saddle point **TS6** associated with this process permits an alternative pseudopericyclic process[38] involving one of the lone pairs of the sp^2-hybridized oxygen atom of **Int3** (Figure 2) to be excluded. The activation energy of this sigmatropic shift is lower than the activation energy associated with the first suprafacial [3,3] pericyclic reaction via **TS1** (see above).

From **Int4** the reaction proceeds through a thermal disrotatory electrocyclization to yield 1,3-cyclohexadiene intermediate **Int5** (Scheme 6). The features of saddle point **TS7** associated with this pericyclic step are those expected for a [$\pi 6_d$] process, in which the hydroxyl group $\mathbf{OH^2}$ formed in the previous step is necessarily inward (pseudoaxial) with respect to the C–C bond being formed (Figure 2). It results in destabilizing four-electron torquoelectronic interactions and steric congestion for this transition structure.[39] As a consequence, this step shows a relatively high activation energy, the second highest found in our calculations along the whole reaction coordinate. It is likely that this step and the first one associated with the [3,3] sigmatropic shift via **TS1** (see above) are responsible for the necessity of dielectric heating to complete these reactions. However, the effect of R^2 substituents in more complex substrates (see Scheme 4) is not critical, since these groups will always occupy the outward position in the corresponding [$\pi 6_d$] transition structures (see the stars in Figure 2).[40]

Finally, **Int5** can be subjected to an aromatization process to produce salicylaldehyde, **P1** with concomitant release of a methanol molecule (see Scheme 6, Figure 1 and Figures S4 and S7 of the Supporting Information). In this reaction step, the assistance of one molecule of imidazole is required to achieve a feasible activation energy ($\Delta G^{\ddagger} = 24.1$ kcal mol^{-1}, **TS8-Imz**). This final step is strongly exergonic and irreversible, as would be expected from the high resonance energy of the phenyl group generated in the course of the elimination/aromatization reaction.

An intriguing aspect of these reactions is the formation of methyl benzoates **15** in several polycyclic systems (see above, Scheme 3). Our computational model indicates that methyl benzoate (**P2** in Scheme 7) can be formed via oxatriene **Int7**, which differs with respect to **Int3** in the *E* configuration of the C^1–C^2 double bond. Despite this difference, **Int7** is almost isoenergetic with **Int3**, but its imidazole-assisted formation via **TS9-Imz** or (*Z*)-**Int6** (which in turn involves saddle points **TS10-Imz** and **TS11**, see Figures S9 and S12 of the Supporting Information) is less favored than in the previous case, which is in line with the minor formation of benzoates **15** in most cases (Scheme 3). Beyond **Int7**, the previously described antarafacial [1,7] sigmatropic shift leads to triene **Int8**, disrotatory electrocyclization of which leads in turn to cyclohexadienyl alcohol **Int9**. The relatively high energy of this pericyclic reaction is as expected for a transition structure involving an inward $\mathbf{OH^2}$ group (see the optimized structure of **TS13** in Figure 2). However, once again, R^2 groups in more substituted systems should occupy outward positions, which in general should not

jeopardize this reaction path. Finally, the imidazole-assisted elimination/aromatization step from **Int9** leads to methyl benzoate **P2** with an energy barrier significantly higher than those found for **P1** (see Schemes 6 and 7). This result is in nice agreement with the experimentally found formation of benzoates **15** as minor products, especially in the case of polycyclic systems.

Conclusion

We have developed a catalytic version of the MW-assisted formation of polysubstituted salicylaldehydes from propargyl vinyl ethers. The reaction manifold uses imidazole as the catalyst (10 mol%) to deliver an array of topologically diverse salicylaldehyde scaffolds spanning from simple aromatic monocycles to complex fused polycyclic systems. The reaction is scalable and instrumentally simple to perform, highly regioselective, and symmetry-disrupting: symmetrically substituted PVEs afforded asymmetrically (nonredundant) substituted salicylaldehydes. The preparative value of this transformation has been demonstrated in the five-step synthesis of the benzophenone-derived natural product morintrifolin B. A DFT study on a simplified model was performed. Calculations underpin a domino mechanism comprising a [3,3] propargyl Claisen rearrangement/[1,3]-hydrogen shift/[1,7]-hydrogen shift/6π electrocyclization/aromatization process. The use of imidazole lowers the energy of the two more difficult steps, that is, the 1,3-prototropic rearrangement and the final aromatization step, otherwise energetically very disfavored.

Experimental Section

General remarks

^{1}H NMR and ^{13}C NMR spectra of $CDCl_3$ solutions were recorded at 400 and 100 MHz or at 500 and 125 MHz (Bruker AC 200 and AMX2–500), respectively. MW reactions were conducted in sealed glass vessels (capacity 10 mL) with a CEM Discover MW reactor. FTIR spectra were measured on chloroform solutions with a PerkinElmer Spectrum BX FTIR spectrophotometer. Mass spectra (low-resolution EI/CI) were obtained with a Hewlett-Packard 5995 gas chromatograph/mass spectrometer. High-resolution mass spectra were recorded with a Micromass Autospec mass spectrometer. Microanalyses were performed with a Fisons Instruments EA 1108 carbon, hydrogen, and nitrogen analyzer. Analytical TLC was performed with E. Merck Brinkman UV-active silica gel (Kieselgel 60 F254) on aluminum plates. Flash column chromatography was carried out with E. Merck silica gel 60 (particle size less than 0.020 mm) and appropriate mixtures of ethyl acetate and hexanes, or ethyl acetate and dichloromethane as eluents. All reactions were performed in oven-dried glassware. All starting materials were obtained from commercial suppliers and used as received. PVEs **1v**, **1w**, **1x**, **1y**, and **1z** partially rearranged during the isolation and characterization process, so an alternative procedure was used to prepare **14v**, **14w**, **14x**, **14y**, and **14z** (see below).

Synthesis

Representative procedure for the MW-assisted synthesis of salicylaldehydes from the corresponding propargyl vinyl ethers: synthesis of 1-hydroxy-3-phenyl-5,6,7,8-tetrahydronaphthalene-2-carbaldehyde (14e): Propargyl vinyl ether **1e** (1.0 mmol) and imidazole (0.10 mmol) in dry xylene (1 mL) were placed in a MW closed vial and the solution was irradiated for 1 h in a single-mode MW oven (300 W, 190 °C). After removing the solvent at reduced pressure the products were purified by flash column chromatography (silica gel, *n*-hexane/EtOAc 95/5) to yield **14e** as an amorphous solid (229.6 mg, 91%). ^{1}H NMR (400 MHz, $CDCl_3$, 25 °C): δ = 1.71–1.75 (m, 4H), 2.62–2.65 (m, 2H), 2.68–2.71 (m, 2H), 6.52 (s, 1H), 7.24–7.26 (m, 2H), 7.30–7.35 (m, 3H), 9.67 (s, 1H), 12.27 ppm (s, 1H); ^{13}C NMR (100 MHz, $CDCl_3$, 25 °C): δ = 22.13, 22.25, 22.39, 30.5, 115.3, 122.1, 125.3, 127.9, 128.2 (2C), 130.0 (2C), 137.8, 143.6, 147.3, 161.2, 196.6 ppm; IR ($CHCl_3$): $\tilde{\nu}$ = 2939.6, 1635.7, 1617.2, 1559.6, 1405.3, 1366.7, 1299.4 cm^{-1}; LRMS (70 eV) *m/z* (%): 252 (100) [M^+], 251 (42), 234 (30), 233 (18), 223 (12), 165 (17); HRMS (EI-TOF): *m/z* calcd for $C_{17}H_{16}O_2$: 252.1150 [M]$^+$; found: 252.1144.

Representative telescoped procedure for the synthesis of salicylaldehydes 14v, 14w, 14x, 14y, and 14z from the corresponding tertiary propargylic alcohols: synthesis of 1-hydroxy-3-phenyl-9,10-dihydrophenanthrene-2-carbaldehyde (14v): The corresponding propargyl alcohol (1.0 mmol) and DABCO (0.10 mmol) were dissolved in hexane (1 mL); a small amount of CH_2Cl_2 was used if the alcohol did not dissolved well in hexane. Methyl propiolate was slowly added dropwise (1.5 mmol) and the reaction mixture was stirred for 5 min. The reaction mixture was filtered through a short column filled with silica gel with *n*-hexane/EtOAc (60/40). The solvent was evaporated off and the mixture was dissolved in xylenes (1 mL) and transferred to a MW closed vial. Imidazole (0.10 mmol) was added and the reaction mixture was irradiated for 1 h in a single-mode MW oven (300 W, 190 °C). After removing the solvent at reduced pressure the products were purified by flash column chromatography (silica gel, *n*-hexane/EtOAc 95/5) to give **14v** as an amorphous solid (153.2 mg; 51%). ^{1}H NMR (400 MHz, $CDCl_3$, 25 °C): δ = 2.89–2.93 (m, 2H), 2.97–3.01 (m, 2H), 7.28–7.34 (m, 4H), 7.42–7.51 (m, 5H), 7.76–7.79 (m, 1H), 9.83 (s, 1H), 12.36 (s, 1H) ppm; ^{13}C NMR (100 MHz, $CDCl_3$, 25 °C): δ 19.8, 28.1, 116.7, 117.0, 124.4, 124.9, 127.0, 128.1, 128.39 (2C), 128.41, 129.2, 130.1 (2C), 133.1, 138.0, 138.6, 142.1, 145.4, 160.1, 196.6 ppm; IR ($CHCl_3$): $\tilde{\nu}$ = 2945.1, 2896.7, 2844.7, 1633.7, 1617.8, 1545.8, 1479.8, 1400.2, 1363.5, 1331.6, 1307.2, 1288.7, 1239.0 cm^{-1}; LRMS (70 eV): *m/z* (%): 300 (100) [M^+], 299 (41), 282 (27), 281 (32), 253 (16), 252 (21), 239 (12), 165 (15). HRMS (EI-TOF): *m/z* calcd for $C_{21}H_{16}O_2$: 300.1150 [M]$^+$; found: 300.1142. Further elution delivered pure methyl 3-phenyl-9,10-dihydrophenanthrene-2-carboxylate (**15v**) as an amorphous solid (31.4 mg; 10%). ^{1}H NMR (400 MHz, $CDCl_3$, 25 °C): δ = 2.93 (br s, 4H), 3.64 (s, 3H), 7.24–7.32 (m, 3H), 7.35–7.44 (m, 5H), 7.33 (d, ^3J(H,H) = 7.1 Hz, 2H), 7.77 ppm (t, ^3J(H,H) = 7.1 Hz, 1H); ^{13}C NMR (100 MHz, $CDCl_3$, 25 °C): δ = 28.5, 28.8, 51.8, 124.2, 126.1, 127.10, 127.12, 127.8 (2C), 128.3, 128.41 (3C), 129.1, 129.7, 133.4, 136.2, 137.4, 137.9, 141.6, 141.7, 168.8 ppm; IR ($CHCl_3$): $\tilde{\nu}$ = 3028.8, 2951.1, 2841.6, 1716.4, 1603.0, 1436.2, 1305.8, 1252.4 cm^{-1}; LRMS (70 eV): *m/z* (%): 314 (57) [M^+], 283 (24), 252 (10), 239 (10), 170 (13), 169 (100), 141 (16), 115 (17), 91(20). HRMS (EI-TOF): *m/z* calcd for $C_{22}H_{18}O_2$: 314.1307 [M]$^+$; found: 314.1305.

Acknowledgements

This research was supported by the Spanish Ministerio de Economía y Competitividad (MINECO) and the European Regional Development Fund (CTQ2011-28417-C02-02 and CTQ2013-45415-P), the UPV/EHU (UFI11/22 QOSYC), and the

Basque Government (GV/EJ, grant IT-324-07). L.C. thanks Spanish MEC for a FPI grant and D.M.A. thanks CSIC for a JAE-intro grant. M.T.-S., M.O.-G., and F.P.C. thank the SGI/IZO- SGIker UPV/EHU and the DIPC for generous allocation of computational resources.

Keywords: domino reactions · microwave chemistry · organocatalysis · synthetic methods · total synthesis

[1] a) D. Tejedor, G. Méndez-Abt, L. Cotos, F. García-Tellado, *Chem. Soc. Rev.* **2013**, *42*, 458 – 471; b) Z.-B. Zhu, S. F. Kirsch, *Chem. Commun.* **2013**, *49*, 2272 – 2283; c) for other reactivity profile, see: D. Tejedor, D. González-Cruz, F. García-Tellado, J. J. Marrero-Tellado, M. L. Rodríguez, *J. Am. Chem. Soc.* **2004**, *126*, 8390 – 8391.

[2] S. Ma, *Chem. Rev.* **2005**, *105*, 2829 – 2871.

[3] D. K. Black, S. R. Landor, *J. Chem. Soc.* **1965**, 6784 – 6788.

[4] a) L. Claisen, *Chem. Ber.* **1912**, *45*, 3157 – 3167 ; b) *The Claisen Rearrangement*, (Eds.: M. Hiersemann, U. Nubbemeyer), Wiley-VCH, Weinheim, **2007**.

[5] a) For the first metal-catalyzed protocol, see: B. D. Sherry, F. D. Toste, *J. Am. Chem. Soc.* **2004**, *126*, 15978 – 15979; For other metal-catalyzed rearrangements, see: b) E. S. da Silva Júnior, N. Maria de Araujo, F. S. Emery, *J. Heterocycl. Chem.* **2015**, *52*, 518 – 521; c) A. Palisse, S. F. Kirsch, *Eur. J. Org. Chem.* **2014**, 7095 – 7098; d) D. V. Vidhani, J. W. Cran, M. E. Krafft, I. V. Alabugin, *Org. Biomol. Chem.* **2013**, *11*, 1624 – 1630; e) H. Huang, H. Jiang, H. Cao, J. Zhao, D. Shi, *Tetrahedron* **2012**, *68*, 3135 – 3144; f) T. Harschneck, S. F. Kirsch, *J. Org. Chem.* **2011**, *76*, 2145 – 2156; g) H. Wei, Y. Wang, B. Yue, P.-F. Xu, *Adv. Synth. Catal.* **2010**, *352*, 2450 – 2454; h) K. Tanaka, E. Okazaki, Y. Shibata, *J. Am. Chem. Soc.* **2009**, *131*, 10822 – 10823; i) J. T. Binder, S. F. Kirsch, *Org. Lett.* **2006**, *8*, 2151 – 2153; j) H. Menz, S. F. Kirsch, *Org. Lett.* **2006**, *8*, 4795 – 4797; k) B. D. Sherry, L. Maus, B. N. Laforteza, F. D. Toste, *J. Am. Chem. Soc.* **2006**, *128*, 8132 – 8133; l) M. H. Suhre, M. Reif, S. F. Kirsch, *Org. Lett.* **2005**, *7*, 3925 – 3927; for selected examples of Claisen rearrangements of *N*-propargyl amines, see: m) A. Saito, A.i Kanno, Y. Hanzawa, *Angew. Chem. Int. Ed.* **2007**, *46*, 3931 – 3933; *Angew. Chem.* **2007**, *119*, 4005 – 4007; n) A. Saito, S. Oda, H. Fukaya, Y. Hanzawa, *J. Org. Chem.* **2009**, *74*, 1517 – 1524.

[6] For selected examples of all-sp^2 C_5 building blocks, see: a) D. V. Vidhani, M. E. Krafft, I. V. Alabugin, *J. Org. Chem.* **2014**, *79*, 352 – 364; b) D. V. Vidhani, M. E. Krafft, I. V. Alabugin, *Org. Lett.* **2013**, *15*, 4462 – 4465; c) T. Sakaguchi, Y. Okuno, Y. Tsutsumi, H. Tsuchikawa, S. Katsumura, *Org. Lett.* **2011**, *13*, 4292 – 4295; d) C. D. Vanderwal, *J. Org. Chem.* **2011**, *76*, 9555 – 9567 and references cited therein.

[7] The parent PVEs armed with an ester or tertiary amide at the propargylic position are synthesized by the tertiary amine catalyzed ABB′ three-component reaction between a 1,2-ketoester (1,2-ketoamide) and methyl propiolate. D. Tejedor, A. Santos-Expósito, F. García-Tellado, *Chem. Eur. J.* **2007**, *13*, 1201 – 1209. For a tutorial review of ABB′ three-component reactions, see: D. Tejedor, F. García-Tellado, *Chem. Soc. Rev.* **2007**, *36*, 484 – 491.

[8] D. Tejedor, L. Cotos, F. García-Tellado, *Org. Lett.* **2011**, *13*, 4422 – 4425.

[9] D. Tejedor, G. Méndez-Abt, L. Cotos, M. A. Ramirez, F. García-Tellado, *Chem. Eur. J.* **2011**, *17*, 3318 – 3321.

[10] D. Tejedor, L. Cotos, F. García-Tellado, *J. Org. Chem.* **2013**, *78*, 8853 – 8858.

[11] a) M. Hasegawa, F. Ono, S. Kanemasa, *Tetrahedron Lett.* **2008**, *49*, 5220 – 5223; b) C. Palomo, R. Pazos, M. Oiarbide, J. M. Garcia, *Adv. Synth. Catal.* **2006**, *348*, 1161 – 1164; c) T. P. Yoon, E. N. Jacobsen, *Angew. Chem. Int. Ed.* **2005**, *44*, 466 – 468; *Angew. Chem.* **2005**, *117*, 470 – 472; d) L. M. Weinstock, S. Karady, F. E. Roberts, A. M. Hoinowski, G. S. Brenner, T. B. K. Lee, W. C. Lumma, M. Sletzinger, *Tetrahedron Lett.* **1975**, *16*, 3979 – 3982.

[12] D. Tejedor, G. Méndez-Abt, L. Cotos, F. García-Tellado, *Chem. Eur. J.* **2012**, *18*, 3468 – 3472.

[13] a) *Coumarins: Biology, Applications and Mode of Action*, (Eds.: R. O. Kennedy, R. D. Thornes), Wiley, New York, **1997**; b) *Flavonoids: Chemistry, Biochemistry and Applications*, (Eds.: O. M. Andersen, K. R. Markham), CRC, Boca Raton, **2006**; c) A. Gaspar, M. J. Matos, J. Garrido, E. Uriarte, F. Borges, *Chem. Rev.* **2014**, *114*, 4960 – 4992; d) R. Pratap, V. J. Ram, *Chem. Rev.* **2014**, *114*, 10476 – 10526; e) Salicylaldehydes rearrange to catechols under oxidative conditions (Dakin rearrangement). For a selected recent example, see: S. Chen, M. S. Hossain, F. W. Foss, *Org. Lett.* **2012**, *14*, 2806–2809 and references cited therein; f) S. Bräse, A. Encinas, J. Keck, C. F. Nising, *Chem. Rev.* **2009**, *109*, 3903 – 3990.

[14] For selected reviews, see: a) K. C. Gupta, A. K. Sutar, *Coord. Chem. Rev.* **2008**, *252*, 1420 – 1450; b) J. F. Larrow, E. N. Jacobsen, *Top. Organomet. Chem.* **2004**, *6*, 123 – 152; c) T. Katsuki, *Chem. Soc. Rev.* **2004**, *33*, 437 – 444.

[15] a) H. Wynberg, *Comp. Org. Syn.* **1991**, *2*, 769 – 775; b) J. C. Duff, E. J. Bills, *J. Chem. Soc.* **1934**, 1305 – 1308; c) For a representative example with preparative value: J. F. Larrow, E. N. Jacobsen, *Org. Synth.* **1998**, *75*, 1 – 11.

[16] G. Cozzi, *Chem. Soc. Rev.* **2004**, *33*, 410 – 421.

[17] Y. Deng, Y. W. Chin, H. Chai, W. J. Keller, A. D. Kinghorn, *J. Nat. Prod.* **2007**, *70*, 2049 – 2052.

[18] For a recent review, see: R. A. Sheldon, *Chem. Soc. Rev.* **2012**, *41*, 1437 – 1451.

[19] The scope of the synthesis of salicylaldehydes **9** from PVEs is further demonstrated in our initial communication.[9,10]

[20] a) D. A. Alonso, C. Nájera, I. M. Pastor, M. Yus, *Chem. Eur. J.* **2010**, *16*, 5274 – 5284; b) J. H. P. Tyman, in *Synthetic and Natural Phenols*, Elsevier, New York, **1996**; c) Z. Rappoport, in *The Chemistry of Phenols*, Wiley-VCH, Weinheim, **2003**.

[21] a) A. Estévez-Braun, A. G. González, *Nat. Prod. Rep.* **1997**, *14*, 465 – 475; b) F. Borges, F. Roleira, N. Milhazes, L. Santana, E. Uriarte, *Curr. Med. Chem.* **2005**, *12*, 887 – 916; c) A. Behrenswerth, N. Volz, J. Toräng, S. Hinz, S. Bräse, C. E. Müller, *Bioorg. Med. Chem.* **2009**, *17*, 2842 – 2851; d) E. Jijy, P. Prakash, M. Shimi, P. M. Pihko, N. Joseph, K. V. Radhakrishnan, *Chem. Commun.* **2013**, *49*, 7349 – 7351.

[22] For example, 5-hydroxylated coumarins (position C^5 in coumarins correlates with position C^6 in the parent salicylaldehyde) are endowed with potent nematicidal activity against the phytopathogenic nematode *Bursaphelenchus xylophilus*: K. Takaishi, M. Izumi, N. Baba, K. Kawazu, S. Nakajima, *Bioorg. Med. Chem. Lett.* **2008**, *18*, 5614 – 5617.

[23] See the Supporting Information for their structures and synthesis.

[24] D. Tejedor, S. J. Álvarez-Méndez, J. M. López-Soria, V. S. Martín, F. García-Tellado, *Eur. J. Org. Chem.* **2014**, 198 – 205.

[25] For selected reviews on cyclobutarenes and related compounds, see: a) A. K. Sadana, R. K. Saini, W. E. Billups, *Chem. Rev.* **2003**, *103*, 1539 – 1602; b) G. Mehta, S. Kotha, *Tetrahedron* **2001**, *57*, 625 – 659.

[26] a) E. Marsault, M. L. Peterson, *J. Med. Chem.* **2011**, *54*, 1961 – 2004; b) E. M. Driggers, S. P. Hale, J. Lee, N. K. Terrett, *Nat. Rev. Drug Discovery* **2008**, *7*, 608 – 624.

[27] a) C. M. Marson, *Chem. Soc. Rev.* **2011**, *40*, 5514 – 5533; b) Substituted tetrahydroisoquinolines as β-secretase inhibitors: L. A. Thompson, K. M. Boy, J. Shi, J. E. Macor, A. C. Good, L. R. Marcin, US 20080153868A1; c) Hydroxy-substituted 1,2,3,4-tetrahydroisoquinolines as inhibitors of phenylethanolamine *N*-methyltransferase (PNMT): D. J. Sall, G. L. Grunewald, *J. Med. Chem.* **1987**, *30*, 2208 – 2216.

[28] M. A. Koch, A. Schuffenhauer, M. Scheck, S. Wetzel, M. Casaulta, A. Odermatt, P. Ertl, H. Waldmann, *Proc. Natl. Acad. Sci. USA* **2005**, *102*, 17272 – 17277.

[29] S. Baggett, E. P. Mazzola, E. J. Kennelly, in *Studies in Natural Products Chemistry, Vol. 32*, Part L, (Ed.: Atta-ur-Rahman), Elsevier, Amsterdam, **2005**, pp. 721.

[30] S.-B. Wu, C. Long, E. Kennelly, *Nat. Prod. Rep.* **2014**, *31*, 1158 – 1117.

[31] O. Potterat, M. Hamburger, *Planta Med.* **2007**, *73*, 191 – 199.

[32] a) R. E. Plata, D. A. Singleton, *J. Am. Chem. Soc.* **2015**, *137*, 3811 – 3826; b) A. Winter, *Nat. Chem.* **2015**, *7*, 413 – 415.

[33] A. D. Becke, *J. Chem. Phys.* **1993**, *98*, 5648 – 5652.

[34] a) W. J. Hehre, R. Ditchfield, J. A. Pople, *J. Chem. Phys.* **1972**, *56*, 2257 – 2261; b) W. J. Hehre, L. Radom, P. von R. Schleyer, J. A. Pople, in *Ab Initio Molecular Orbital Theory*, Wiley, New York, **1986**.

[35] a) K. Ishida, K. Morokuma, A. Kormornicki, *J. Chem. Phys.* **1977**, *66*, 2153 – 2156; b) C. Gonzalez, H. B. Schlegel, *J. Chem. Phys.* **1989**, *90*, 2154 – 2161; c) C. Gonzalez, H. B. Schlegel, *J. Phys. Chem.* **1990**, *94*, 5523 – 5527.

[36] Y. Zhao, D. G. Truhlar, *Theor. Chem. Acc.* **2008**, *120*, 215 – 241.

[37] Guassian 2009, Revision B.01, M. J. Frisch, G. W. Trucks, H. B. Schlegel, G. E. Scuseria, M. A. Robb, J. R. Cheeseman, G. Scalmani, V. Barone, B.

Mennucci, G. A. Petersson, H. Nakatsuji, M. Caricato, X. Li, H. P. Hratchian, A. F. Izmaylov, J. Bloino, G. Zheng, J. L. Sonnenberg, M. Hada, M. Ehara, K. Toyota, R. Fukuda, J. Haseg-awa, M. Ishida, T. Nakajima, Y. Honda, O. Kitao, H. Nakai, T. Vreven, J. A. Montgomery Jr., J. E. Per-alta, F. Ogliaro, M. Bearpark, J. J. Heyd, E. Brothers, K. N. Kudin, V. N. Staroverov, R. Kobayashi, J. Normand, K. Raghavachari, A. Rendell, J. C. Burant, S. S. Iyengar, J. Tomasi, M. Cossi, N. Rega, J. M. Millam, M. Klene, J. E. Knox, J. B. Cross, V. Bakken, C. Adamo, J. Jaramillo, R. Gomperts, R. E. Stratmann, O. Yazyev, A. J. Austin, R. Cammi, C. Pomelli, J. W. Ochterski, R. L. Martin, K. Moroku-ma, V. G. Zakrzewski, G. A. Voth, P. Salvador, J. J. Dannenberg, S. Dapprich, A. D. Daniels, Ö. Farkas, J. B. Foresman, J. V. Ortiz, J. Cioslowski, D. J. Fox, Gaussian, Inc., Wallingford CT, **2010**.

[38] a) P. von R. Schleyer, J. I. Wu, F. P. Cossío, I. Fernández, *Chem. Soc. Rev.* **2014**, *43*, 4909 – 4921; b) D. Martin Birney, *Curr. Org. Chem.* **2010**, *14*, 1658 – 1668.

[39] a) J. D. Evanseck, B. E. Thomas IV, D. C. Spellmeyer, K. N. Houk, *J. Org. Chem.* **1995**, *60*, 7134 – 7141; b) V. A. Guner, K. N. Houk, I. W. Davies, *J. Org. Chem.* **2004**, *69*, 8024 – 8028; c) T.-Q. Yu, Y. Fu, L. Liu, Q.-X. Guo, *J. Org. Chem.* **2006**, *71*, 6157 – 6164.

[40] Another conceivable reaction mechanism involves the formation of a furan intermediate (see Scheme S1 and Figure S14 in the Supporting Information). This mechanism was discarded on the basis of its global free-energy barrier of 57.5 kcal mol^{-1} with respect to **R**.

Received: August 11, 2015
Published online on October 30, 2015